

B. Belleville<sup>1</sup>, T. Stevanovic<sup>1\*</sup>, A. Cloutier<sup>1</sup>, A. Pizzi<sup>2</sup>, A. Salenikovich<sup>1</sup>, and P. Blanchet<sup>1,3</sup>

Production and properties of wood-welded panels made from two Canadian hardwoods

<sup>1</sup> Centre de recherche sur le bois, Département des sciences du bois et de la forêt, Faculté de foresterie, de géographie et de géomatique, Université Laval, 2425 rue de la Terrasse, Québec, QC, G1V 0A6, Canada

<sup>2</sup> ENSTIB-LERMAB, Université Henri Poincaré, Nancy 1, 27 rue du Merle Blanc, BP 1041, 88051 Épinal, France

<sup>3</sup> FPInnovations, 319 rue Franquet, Québec, QC, G1P 4R4, Canada

The authors are, respectively, PhD candidate, Professor, Professor and Associate Professor, Centre de recherche sur le bois, Département des sciences du bois et de la forêt, Univ. Laval, Québec, Canada (benoit.belleville.1@ulaval.ca, Tatjana.Stevanovic@sbf.ulaval.ca, Alain.Cloutier@sbf.ulaval.ca, Alexander.Salenikovich@sbf.ulaval.ca); Professor, ENSTIB-LERMAB, Univ. Henri Poincaré, Nancy 1, France (antonio.pizzi@enstib.uhp-nancy.fr); Group Leader, FPInnovations, Québec, Canada, and Adjunct Professor, Centre de recherche sur le bois, Département des sciences du bois et de la forêt, Univ. Laval, Québec, Canada (pierre.blanchet@fpinnovations.ca).

\*Corresponding author: Tel.: (+1) 418 656-2131 #7337; Fax: (+1) 418 656-2091.

## **Abstract**

This study examines the suitability of wood welding technology for producing composite panels for furniture applications with two Canadian hardwood species, sugar maple (*Acer saccharum*) and yellow birch (*Betula alleghaniensis*). For each species, twelve 30x225x300 mm panels were manufactured using a panelling machine specifically designed for rotational wood-dowel welding with optimized parameters obtained from a previous study. Six edge-glued panels of the same size were manufactured from each species using a non-structural polyvinyl acetate (PVA) adhesive and tested for comparative purposes. The experimental program included three-point bending at 255-mm span and visual inspection of the panels to assess performance at standard moisture conditions and after an aging cycle with variable relative humidity. Average breaking load of 1.79 kN and 1.70 kN was obtained at standard moisture conditions for welded panels of yellow birch and sugar maple, respectively. Fractures consistently occurred in the dowel's cross-section, whereas no slippage was observed along the welded interface. Delamination between wood slats occurred after the aging cycle, but did not affect the bending properties. Results confirm the suitability of wood-dowel welding for producing furniture panelling with Canadian hardwood species. Further research is needed to design panels with a more efficient position and use of welded dowels and with panel product properties that are comparable or superior to those of glued counterparts.

**Keywords:** sugar maple, yellow birch, rotational wood-dowel welding, three-point bending, wood-welded panel, furniture, eco-conception

## 1. Introduction

Rotational wood-dowel welding without an adhesive has recently been shown to rapidly produce wood joints of considerable strength (Pizzi et al. 2004; Ganne-Chedéville et al. 2005; Kanazawa et al. 2005). Previous studies have investigated structural applications of wood products assembled by dowel welding, such as suspended wood flooring (Bocquet et al. 2007a), mortise and tenon wood joints (Mougel et al. 2011), and laminated wood beams (Bocquet et al. 2007b). Wood furniture joints (Segovia and Pizzi 2009), wood-welded chairs (Renaud 2009), wood-dowel welding in wood composite panels (Resch et al. 2006), and more recently, sustainable wood-welded panels with European species (Belleville et al. 2011) are some other successful product developments.

Rotational wood-dowel welding offers a promising alternative for panelling applications in the furniture industry. Friction between the dowel and substrate during insertion (less than 3 s) combined with high-speed dowel rotation causes the temperature to rise, which induces the lignin to soften and the wood to weld. The usual adhesive used in hardwood panelling is polyvinyl acetate (PVA), which requires long curing time (up to 24 hours) and multiple handling. These constraints limit the production flow and flexibility required for customized production. In addition, wood-dowel welding can reduce the use of petrochemicals, increase productivity, and lower production costs.

Most studies to date on rotational wood-dowel welding have considered European species such as European beech (*Fagus sylvatica*), European ash (*Fraxinus excelsior*), or Scots pine (*Pinus sylvestris*), with less attention paid to North American species. The objectives of the present study were therefore 1) to produce wood-welded panels made from sugar maple (*Acer saccharum*) and yellow birch (*Betula alleghaniensis*), two Canadian hardwood species that are frequently used for indoor appearance products, using a specifically designed panelling machine; 2) to assess the flexural properties of the wood-welded panels, considering the required load-bearing capacity for a typical standard panel used for furniture components; 3) to assess the performance of the wood-welded panels at standard moisture conditions and after humidity cycling; and 4) to compare the flexural properties of the wood-welded panels with those of PVA-glued counterparts.

## 2. Material and methods

### 2.1 Test specimen preparation

All wood material was pre-conditioned in a conditioning room at 20 °C and 60% relative humidity (RH) until constant mass was reached. To prepare panel specimens, 25x30x225 mm slats of sugar maple and yellow birch wood were cut from clear wood material. For each panel, 12 slats were attached by 44 wood-welded dowels to assemble a 30x 225x300 mm panel (Fig. 1). Twelve wood-welded panels per species were assembled and then stored at 20 °C and 60% RH for 7 days prior to testing.

#### 2.1.1. Wood welding parameters

High-speed rotation-induced mechanical friction wood-dowel welding was performed using a panelling machine specifically designed at the *Centre de Recherche Industrielle du Québec*. The

machine included a multi-functional rotational system coupled with a pneumatic supporting device to hold the wood slats together during welding. The multi-functional rotational system was mounted on a vertical shaft and equipped with a drill to bore a hole, a chuck to hold the dowel during insertion, and an end mill to remove the excess dowel. Two welding parameter sets were applied, based on results of our previous study (Belleville et al. 2012): 1000 rpm rotational speed and 25 mm s<sup>-1</sup> insertion speed for sugar maple and 1000 rpm and 16 mm s<sup>-1</sup> for yellow birch.

Plain-shank dowels of sugar maple and yellow birch wood, 9.68 mm in diameter and 96 mm in length, were commercially manufactured by a local supplier. Dowels were welded by inserting them into pre-drilled holes 7.67 mm in diameter and 50 mm deep into two adjacent slats. The same species was used for each dowel and slat combination (Fig. 2). Holes were positioned at 50-mm centre-to-centre distance and 25-mm distance from the end. Each pair of dowels was placed in offset position, with one dowel 5 mm above and the other 5 mm below the centre of the panel. After insertion, the excess dowel was removed with the end mill. Using the same procedure, successive slats were attached using a row of dowels positioned at 25 mm offsets along the length and at staggered vertical positions.

### 2.1.2. Edge-glued panels

Edge-glued panels with identical dimensions to the wood-welded panels were produced for comparative purposes. A cold-set non-structural polyvinyl acetate (PVA) emulsion was used as the adhesive. Glued panels were prepared according to typical industrial assembly parameters and techniques. **The adhesive film thickness was 0.127 mm. The pressure applied was 1.38 MPa for 2 h at 20 °C as suggested by the manufacturer.**

## 2.2 Three-point bending tests

### 2.2.1 Panel bending properties estimation

The normal stress ( $\sigma$ ) distribution in a solid or edge-glued panel under transverse load can be modelled using beam theory. It is assumed that within the elastic limit the compressive and tensile stresses develop in the cross-section of the beam in proportion to the distance from the neutral axis. Fibres in the upper part of the beam are in compression, whereas fibres in the lower part are in tension. Although no data on bending of wood perpendicular to the grain is available in the literature, we can assume the following equation (USDA 2010):

$$E_{90} \cong \frac{E_0}{15.4} \quad [1]$$

The stress distribution in a wood-welded panel under a transverse load is somewhat complex, and potentially similar to that for a reinforced concrete plate: the compressive stress develops in the upper part through the contact between the adjacent slats, whereas the tensile stress in the lower part is resisted by the dowels only (Fig. 3). However, given the geometry of the panel, the dowels in the lower part would not be in simple tension, but instead in a complex stress–strain state. Due to their low slenderness ratio ( $L/D \cong 7$ ) and position in the panel, these dowels would be subjected to combined bending and shear. In the upper part of the panel, the compressive stress

would act perpendicular to the grain of the slats and parallel to the grain of the dowels. Therefore, these dowels would be expected to provide compression reinforcement and to be subjected to combined bending and shear stresses. The stresses would be transferred to the dowels in both parts through the welded interface. The depth of the compression zone and hence the bending properties of the wood-welded panel would depend on 1) the number and vertical positioning of the dowels, 2) the elastic properties of the wood slats (in particular, MOE perpendicular to the grain), 3) the welded bond shear strength, and 4) dowel strength and stiffness. The following model was developed to determine these properties:

The panel's maximum bending stress ( $\sigma_{max}$ ) can be obtained with the following equation:

$$\sigma_{max} = \frac{M}{I} * Y \quad [2]$$

where  $M$  is the bending moment;  $I$  is the moment of inertia; and  $Y$  is the position along the y axis in the section area in which the stress is calculated. The moment of inertia ( $I$ ) for the dowels ( $D_i$ ) and the substrate section between  $D_1$  and the panel's top surface ( $S_1$ ) can be determined from eqs. 3 and 4:

$$I_{d_i} = \frac{\pi d^4}{64} \quad [3]$$

$$I_{S_1} = \frac{Bt_1^3}{12} \quad [4]$$

where  $d$  is the dowel diameter at neighbouring slat junctions (7.67 mm);  $B$  is the panel width (mm); and  $t_1$  **is the depth of the contact area (mm) which can be found by trial and error until equivalent to the distance between the neutral axis (Z) and the panel's top surface.**

$M$  can be calculated using the following equation:

$$M = \frac{P_{max} L}{4} \quad [5]$$

where  $P_{max}$  is the load at break (N) and  $L$  is the span (255 mm).

The position along the y axis in the section area in which the stress is calculated is shown in Fig. 4. Assuming a load concentrated at the centre of the wood-welded panel,  $Z$  can be calculated as follows:

$$Z = \frac{\sum(E_i A_i Y_i)}{\sum(E_i A_i)} \quad [6]$$

where  $E_i$  is the bending properties of component  $i$  (MPa) and  $A_i$  is the section area of component  $i$  ( $\text{mm}^2$ ).

The bending stiffness ( $E_i A_i$ ) for  $S_1$  and  $d_i$  can be obtained from eqs. 7 and 8, respectively.

$$E_{S_1} A_{S_1} = E_{90} A_{S_1} = \frac{E_0}{15.4} * B * t_1 \quad [7]$$

$$E_{d_i} A_{d_i} = E_0 \frac{\pi d^2}{4} N \quad [8]$$

where  $E_{90}$  is the bending properties perpendicular to the grain;  $E_0$  is the bending properties parallel to the grain; and  $N$  is the number of dowels. The effective bending stiffness ( $EI_{eff}$ ) can be calculated using the following equation:

$$EI_{eff} = \sum (E_i I_i + E_i A_i Z_i^2) \quad [9]$$

where  $Z_i$  is the distance between the central axis of an element and the neutral axis, as shown in Fig. 3.

The section modulus ( $S_{eff}$ ) was calculated with eq. 10

$$S_{eff} = \frac{EI_{eff}}{E_i} Z_{D_2} \quad [10]$$

Then  $\sigma_{max}$  can be obtained with eq. 11

$$\sigma_{max} = \frac{M * E_i}{EI_{eff}} Z_{D_2} \quad [11]$$

and introducing eqs. 5 and 10 into eq. 11, eq. 12 is obtained:

$$\sigma_{max} = \frac{M}{S_{eff}} = \frac{L P_{max}}{4 S_{eff}} \quad [12]$$

Based on the static bending properties for each species (Jessome 2000),  $P_{max}$  for yellow birch and sugar maple wood-welded panels would be 2117 and 2297 N, respectively.

### 2.2.2 Panel bending properties determination

Panels were subjected to three-point bending tests using a universal testing machine (MTS QT 5 KN) based on ASTM D1037 (ASTM 2006) (Fig. 5). The test procedure was slightly modified to account for panel thickness and the manufacturing equipment used (span-depth ratio: 8.5). The

load ( $P$ ) was applied at the centre of the panel under a constant  $2 \text{ mm min}^{-1}$  head displacement and 255-mm span ( $S$ ). The first panel of each series was tested until fracture to determine  $P_{max}$ . Five panels for each series were then tested at the same speed but according to a loading program: once 0.4 of the predetermined  $P_{max}$  was reached, the load was decreased to  $0.1 P_{max}$  for 30 s and then increased until panel rupture occurred. Panel deflection was calculated with TestWorks 4.11 B. A linear regression of the load-deflection curve ( $\Delta F/\Delta \delta$ ) from 0.1 to 0.4 of  $P_{max}$  was calculated. The slope of the resulting linear elastic portion of this curve provided valuable information on panel stiffness.

### 2.3 Humidity cycle

Panels were tested according to a specifically developed protocol for indoor wood-composite panels in North American conditions (Blanchet et al. 2003). The humidity cycling test provides valuable information on wood-welded panel delamination under typical Canadian climate changes. Six wood-welded and three PVA-glued panels were assembled for each species. Panels were varnished with a 95% gloss precatalyzed clear lacquer to facilitate visual inspection and pre-conditioned at  $20 \text{ }^\circ\text{C}$  and 60% RH. Panels were then submitted to a relative humidity cycling test (Fig. 6) and then visually inspected. Cycling conditions were: 1)  $20 \text{ }^\circ\text{C}$  and 80% RH for 24 h; 2)  $20 \text{ }^\circ\text{C}$  and 20% RH for 24 h; 3)  $20 \text{ }^\circ\text{C}$  and 80% RH for 72 h; and 4)  $20 \text{ }^\circ\text{C}$  and 20% RH for 72 h. The visual inspection aimed to detect delamination and/or distortion in the panels. After humidity cycling, the wood-welded panels were again stored at  $20 \text{ }^\circ\text{C}$  and 60% RH for 14 days prior to static bending testing, as described above.

## 3. Results and discussion

### 3.1 Three-point bending tests

Test results at standard moisture conditions and after humidity cycling are presented in Table 1. Wood-welded panels showed failure in the joints at the midspan of the panel or in the lamination next to it (Fig. 7). Fractures consistently occurred as splintering tension in the dowels (ASTM 2009), which usually occurs in wood at low moisture content (Bodig and Jayne 1993). No slippage was observed along the welded interface. Signs of compression deformation perpendicular to the grain were occasionally observed in the upper part of the wood slats (above  $D_1$ ), indicating that the welded dowel joint was not the weakest element, and therefore did not have the greatest effect on panel stiffness.

The average  $P_{max}$  at standard moisture conditions was slightly higher for yellow birch (1.79 kN) than for sugar maple (1.70 kN), although the difference was not statistically significant ( $\alpha = 0.05$ ). Better overall elastic stiffness results were obtained for sugar maple wood-welded panels ( $0.37 \text{ kN mm}^{-1}$ ) than for yellow birch ( $0.34 \text{ kN mm}^{-1}$ ). However, no significant difference in  $P_{max}$  ( $\alpha = 0.05$ ) was found between species. The average deflection at  $P_{max}$  for wood-welded panels was 11.1 mm for sugar maple and 14.0 mm for yellow birch.

The elastic stiffness and bending strength results were significantly higher for glued than for wood-welded panels. The dowel's cross-section area, where the stresses were concentrated, was significantly smaller than the edge-glued surface, and dowel placement appeared to be inefficient for the applied load. Results are in accord with those of Vallée et al. (2012) who stated that the load transfer in wood welded joints could be conceptually comparable to adhesively bonded joints with an efficient panel design. As observed previously with wood-welded panels, species was not an influential factor for the mechanical properties of edge-glued panels. The average  $P_{max}$  and elastic stiffness of PVA-glued panels was 5.75 kN and 1.52 kN mm<sup>-1</sup> for sugar maple and 5.21 kN and 0.98 kN mm<sup>-1</sup> for yellow birch, respectively. The average deflection at fracture for glued sugar maple panels (3.9±1.1 mm) was significantly lower than for yellow birch (6.2±0.8 mm).

Typical load-deflection profiles for wood-welded and edge-glued panels are presented in Fig. 8. **Deflection in wood-welded panels was relatively high compared to edge-glued panels, approximately (15 mm and 5 mm, respectively). The elastic limit for both wood-welded and edge-glued panels appeared to be around 4 to 5 mm deflection. While the behaviour of an edge-glued panel was brittle due to rupture of the wood fibers in tension at the bottom, the wood-welded panels showed large plastic deformation beyond the elastic limit (as shown in Fig. 8), which corresponds approximately to the stress at proportional limit perpendicular to grain at the upper face of the panel; i.e., at 9.72 MPa and 7.24 MPa for sugar maple and yellow birch, respectively, according to Jessome (2000). Large deflection occurring in wood-welded panel can be explained by the fact that the bottom parts of the wood slats were not welded and were free to separate during the bending test. Plastic deformation and crushing of the fibers in the upper part of the panel would also translate in a wider gap at the bottom of the panel as bending test progress. The plastic deformation would continue until the rupture of the wood-welded dowels. The dowels ultimately splintered when their tension strength was exceeded, corresponding to a load of roughly 2 kN as depicted in Fig. 8.**

The estimated mechanical properties were higher than the experimentally determined properties for both species. This difference could be due to the wood material density or quality. Wood material density (oven-dry mass/saturated volume) was measured following testing. Results showed lower wood material density than reported in the literature for both species (Jessome 2000). The biggest difference compared to the literature was found for wood dowels (birch: 494±30 kg per cubic meter; maple: 545±70 kg per cubic meter). In fact, commercially manufactured wood dowels are generally made from wood residuals and/or lesser quality tree sections, with lower mechanical attributes than standard clear wood material. This material could also be more heterogeneous and anisotropic than clear wood.

The use of beam theory in the analysis is also an approximation, given the complex interaction between the material properties and the geometry of the welded panel. The development of a numerical model using the finite element method coupled with additional tests on more panels with various configurations (e.g., dowel spacing and/or vertical positioning) could allow a more efficient validation and optimization of the experimental and estimated results. Further research is needed to optimize the panel design, including placement of the wood-welded dowels so that the properties of the produced panel are comparable or superior to its glued counterpart.

At equilibrium, wood-welded panels from both species yielded statistically similar bending properties. However, different behaviour was noted following humidity cycling. After aging cycles with variable humidity, the average  $P_{max}$  was significantly affected by species, with sugar maple (2.13 kN) providing better bending properties than yellow birch (1.82 kN). As observed above, the average deflection at failure for sugar maple (9.2 mm) wood-welded panels was lower than for yellow birch (13.1 mm). The elastic stiffness of yellow birch and sugar maple wood-welded panels was 0.34 and 0.45 kN mm<sup>-1</sup>, respectively. Bending properties of sugar maple wood-welded panels improved significantly from an initial  $P_{max}$  and  $\Delta F/\Delta\delta$  ratio of 1.70 kN and 0.37 kN mm<sup>-1</sup> to 2.13 kN and 0.45 kN mm<sup>-1</sup> following the relative humidity cycling. The humidity cycling did not affect the  $P_{max}$  or the  $\Delta F/\Delta\delta$  ratio for yellow birch wood-welded panels (from 1.79 kN and 0.34 kN mm<sup>-1</sup> to 1.82 kN and 0.34 kN mm<sup>-1</sup>).

Panel bending properties after relative humidity cycling were species dependent, which was not the case at equilibrium. Although  $P_{max}$  improved for both species, differences were significant only for sugar maple. The most plausible explanation is tangential swelling, which was greater for sugar maple than for yellow birch (Jessome 2000). Dowel swelling following the hygrometric cycle would provide a better contact between the dowel and substrate at the welded interface and improve the panel's bending properties. These results could also be explained by sorption hysteresis, caused by the desorption of active sorption sites along cellulose chains that form hydrogen bonds with each other as they lose water. During subsequent adsorption, the surface is subjected to a compressive stress that lowers the equilibrium moisture content. In addition, some of the hydrogen bonds between the chains will not break until the fibres reach saturation, which is followed by another desorption step (Siau 1995). A further possibility, albeit somewhat less likely, is the high concentration of fatty acids and other lipophylic extractives in yellow birch (Dahm 1967; Lavoie and Stevanovic 2005) compared to sugar maple (Rowell 1984). Birch wood is rich in triterpenes and lipophylic extracts such as long chain fatty acids and sterols, which tend to migrate following temperature treatment (Stevanovic and Perrin 2009). The hydrophobic nature of extracts limits water adsorption in wood material. Hemingway (1969) reported reduced yellow birch wettability after thermal treatment from 105 to 220 °C. The temperature increase during welding of yellow birch wood could cause lipophylic components at the welded interface to migrate. A high concentration of those components at the welded zone would prevent water vapour from migrating to or from the welded interface during the conditioning cycle, and therefore limit swelling. This could explain the behaviour of yellow birch after the hygrometric cycle.

### 3.2 Panel appearance after humidity cycling

Wood-welded and glued panels were submitted to humidity cycling to assess the appearance and delamination of aged panels. Dimensional stability is an essential requirement for appearance products. Residual stresses related to manufacturing processes or to nonhomogeneous water vapour adsorption and desorption in service could induce distortion and consequently decrease product value. The objective was to confirm that wood-welded panels would retain their initial appearance after exposure to variable hygrometric conditions in service. No distortion was observed after the humidity cycles for both wood-welded and glued panels. Edge separation along

the length of some wood-welded panels was observed after the first step at 20 °C and 20% RH for 24 h. This can be explained by wood slat shrinkage in response to dry conditions. When the panels were reconditioned at 20 °C and 80% RH for 72 h, the splits previously observed at 20% RH disappeared due to wood swelling under moist hygrometric conditions, but reappeared in wood-welded panels and initially appeared in glued panels after the final 72-h step at 20 °C and 20% RH. Deeper separation of slats in the space between the dowels was observed in wood-welded panels. Edge separation also occurred in glued panels at this point in the humidity cycling. After the final 72-h step at 20 °C and 80% RH, panels regained their original appearance. Wood-welded panels retained their solidity throughout the cycle. However, the improved assembling technique (e.g., wood slats held under pressure during welding) and the adjustments to the wood material MC before welding would be required to keep delamination splitting to a minimum during the panel's life cycle. Edge separation of unglued edges due to variations in moisture conditions could also be minimized with a surface finishing treatment (i.e. varnish) to reduce moisture sorption.

#### **4. Conclusions**

The main objective of this study was to assess the suitability of wood welding technology for producing composite panels for furniture applications made with two Canadian hardwood species, sugar maple and yellow birch. Wood-welded panel specimens were produced with a specifically designed panelling machine, tested, and compared with PVA edge-glued counterparts. The behaviour of wood-welded panels in standard moisture conditions and after an aging cycle with variable humidity was also investigated.

Wood-welded panel bending properties were not affected by wood species, with average load at break of 1.79 kN and 1.70 kN for yellow birch and sugar maple, respectively. Fractures consistently occurred in the dowels as splintering tension, and no slippage was observed along the welded interface. From this perspective, the welded dowel joint was not the weakest element, and therefore did not have the greatest effect on panel stiffness. The bending properties of the wood-welded panel appeared to depend on performance criteria such as the number and vertical positioning of the dowels, the elastic properties of the wood slats, the welded bond shear strength, and the strength and stiffness of the dowels. Further research is needed to design panel configurations with more efficient placement and use of wood-welded dowels in order to produce panel products with properties that are comparable or superior to those of their glued counterparts. The development of a numerical model could help shed light on the mechanics of wood-welded panels submitted to a bending effort. Combined with a sensitivity analysis, such models could help optimize the design parameters.

No distortion was observed in wood-welded panels following humidity cycling. The cycling did not negatively affect the panel's bending properties. Edge splitting was observed in both wood-welded and glued panels due to wood slat shrinkage in response to dry conditions. Additional work and/or special treatment on the panel surface is needed to improve the technique and to minimize splitting throughout the product life cycle.

Rotational wood-dowel welding of North American wood species provides a promising alternative to gluing. The results confirm that wood-dowel welding could be suitable for

producing panels from certain North American species. The technique could help improve production flow and flexibility by eliminating long curing times for adhesive polymerization as well as multiple handling. Moreover, manufacturers would no longer need to buy or store petrochemically derived adhesives. Furthermore, because welded panels are made entirely of wood, they are also fully and easily recyclable.

### **Acknowledgements**

The authors acknowledge the financial support of Le Fonds Québécois de la Recherche sur la Nature et les Technologies for a research grant, the Natural Sciences and Engineering Research Council of Canada, and FPInnovations for a scholarship (B. Belleville). Thanks are extended to the Centre de Recherche Industrielle du Québec and EQMBO Entreprises for technical support.

## Literature Cited

- American Society for Testing and Materials (2009) Standard test methods for small clear specimens of timber. ASTM D143. ASTM, West Conshohocken, PA, USA.
- American Society for Testing and Materials (2006) Standard test methods for evaluating properties of wood-base fiber and particle panel materials. D1037. ASTM, West Conshohocken, PA, USA.
- Belleville B, Stevanovic T, Pizzi A, Cloutier A, Blanchet P (2012) Determination of optimal wood-dowel welding parameters for two North American hardwood species. *J Adhes Sci Technol* (in Press).
- Belleville B, Segovia C, Pizzi A, Stevanovic T, Cloutier A (2011) Wood blockboards fabricated by rotational dowel welding. *J Adhes Sci Technol* 25(20): 2745-2753.
- Blanchet P, Beauregard R, Cloutier A, Gendron G, Lefebvre M (2003) Evaluation of various engineered wood parquet flooring constructions. *For Prod J* 53(1): 89-93.
- Bocquet J-F, Pizzi A, Resch L (2007a) Full-scale industrial wood floor assembly and structures by welded-through dowels. *Holz Roh Werkst* 65(2): 149-155.
- Bocquet J-F, Pizzi A, Despres A, Mansouri HR, Resch L, Michel D, Letort F (2007b) Wood joints and laminated wood beams assembled by mechanically-welded wood dowels. *J Adhes Sci Technol* 21(3-4): 301-317.
- Bodig J, Jayne BA (1993) *Mechanics of Wood and Wood composites*. Krieger Publishing Company, FLO, USA. 712 p.
- Dahm HP (1967) Birchwood as raw material for pulping. II. Stored wood. *Norcks Skogind* 21: 10-14.
- Ganne-Chedéville C, Pizzi A, Thomas A, Leban J-M, Bocquet J-F, Despres A, Mansouri HR (2005) Parameter interactions in two-block welding and the wood nail concept in wood dowel welding. *J Adhes Sci Technol* 19(13/14): 1157-1174.
- Hemingway RW (1969) Thermal instability of fats relative to surface wettability of yellow birch wood (*Betula lutea*). *Tappi J* 52(11): 2149-2155.
- Jessome AP (2000) *Strength and Related Properties of Woods Grown in Canada*. Forintek Canada Corp., Special Publication SP514E. Sainte-Foy, Canada. 37 p.
- Kanazawa F, Pizzi A, Properzi M, Delmotte L, Pichelin F (2005) Parameters influencing wood-dowel welding by high-speed rotation. *J Adhes Sci Technol* 19(12): 1025-1038.
- Lavoie J-M, Stevanovic T (2005) Variation of chemical composition of the lipophilic extracts from yellow birch (*Betula alleghaniensis*) foliage. *J Agric Food Chem* 53(12): 4747-4756.

Mougel E, Segovia C, Pizzi A, Thomas A (2011) Shrink-fitting and dowel welding in mortise and tenon structural wood joints. *J Adhes Sci Technol* 25(1-3): 213-221.

Pizzi A, Leban J-M, Kanazawa F, Properzi M, Pichelin F (2004) Wood dowel bonding by high speed rotation welding. *J Adhes Sci Technol* 18(11): 1263-1278.

Renaud A (2009) Minimalist Z chair assembly by rotational dowel welding. *Eur J Wood Wood Prod* 67(1): 111-112.

Resch L, Despres A, Pizzi A, Bocquet J-F, Leban J-M (2006) Welding-through doweling of wood panels. *Holz Roh Werkst* 64(5): 423-425.

Rowell R (1984) *The chemistry of solid wood*. American Chemical Society, Washington, USA. 618 p.

Segovia C, Pizzi A (2009) Performance of dowel-welded wood furniture linear joints. *J Adhes Sci Technol* 23(9): 1293-1301.

Siau JF (1995) *Wood: Influence of moisture on physical properties*. Department of Wood Science and Forest Products, Virginia Polytechnic Institute and State University, Virginia, USA, 227 p.

Stevanovic T, Perrin D (2009) *Wood chemistry*. Presses polytechniques et universitaires romandes. France. 248 p. (In French).

US Department of Agriculture (USDA) (2010) *Wood Handbook: Wood as an Engineering Material*. USDA Forest Service, Forest Products Society, WI, USA. 508 p.

Vallée T, Tannert T, Ganne-Chedéville C (2012) Capacity prediction of welded timber joints. *Wood Sci Technol* 46: 333-347.

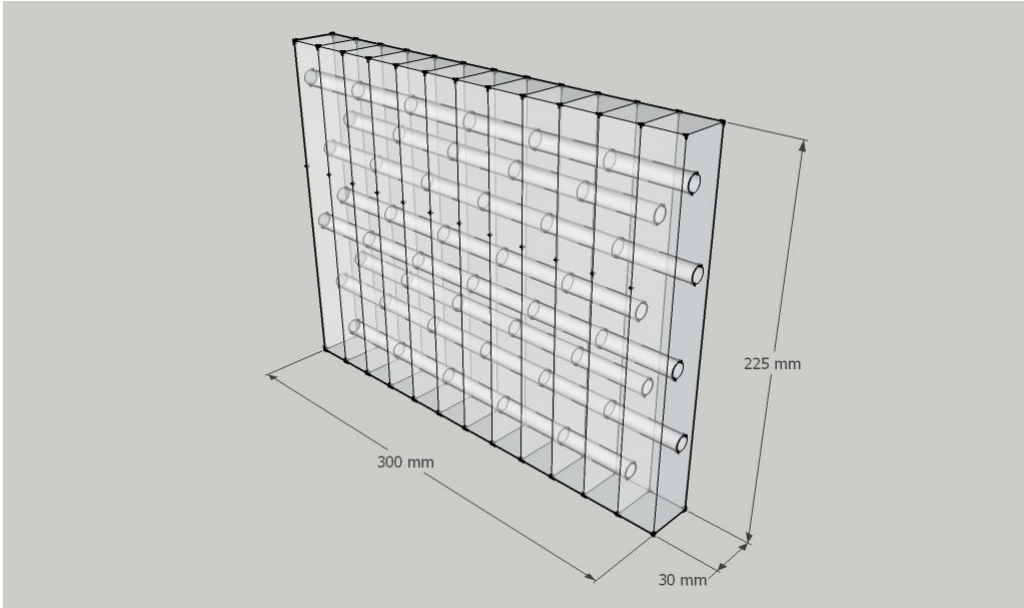


Fig. 1 Schematic view of a wood-welded panel.



Fig. 2 Cross-cut wood dowel welded through two wood slats.

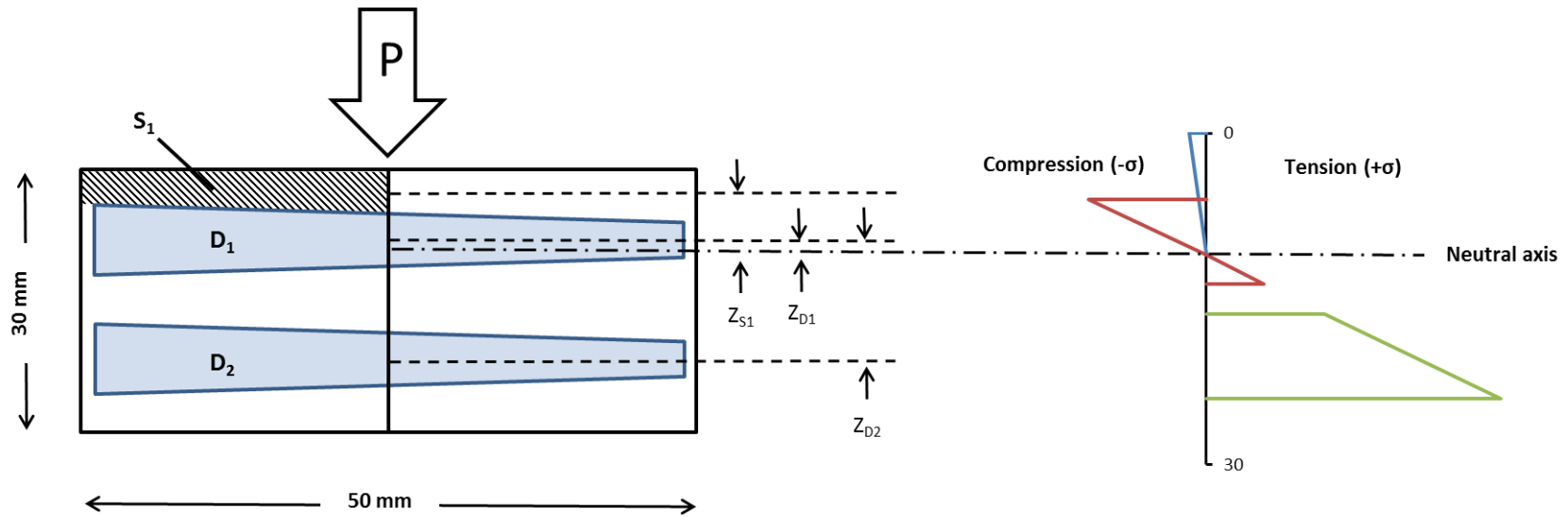


Fig 3 Schematic view and stress distribution in two wood slats held together by two wood-welded dowels ( $D_1$  and  $D_2$ ) tested in three-point bending.  $S_1$ : substrate section between  $D_1$  and the panel's top surface (hatched);  $P$ : load;  $\sigma$ : bending stress;  $Z_i$ : distance between the central axis of an element and the neutral axis.

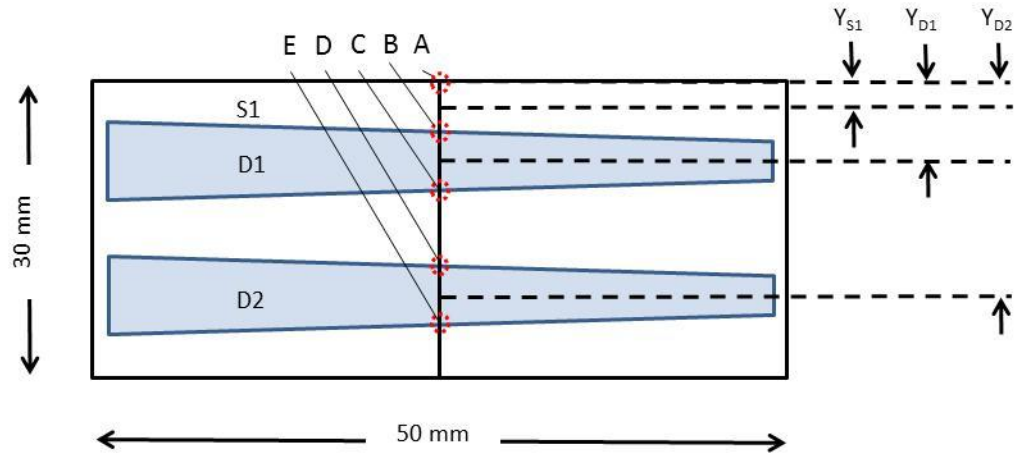


Fig. 4 Schematic view of two wood-welded dowels ( $D_1$  and  $D_2$ ) holding two wood slats together.  $Y_i$ : position along the  $Y$  axis on the section area in which the stress is calculated;  $S_i$ : substrate section between  $D_1$  and the panel's top surface; A to E: Distance (mm) from surface (point A) of a specific point inside the wood-welded panel (A: 0; B: 6; C: 13.67; D: 16.33; E: 24).



Fig 5 Three-point bending test.

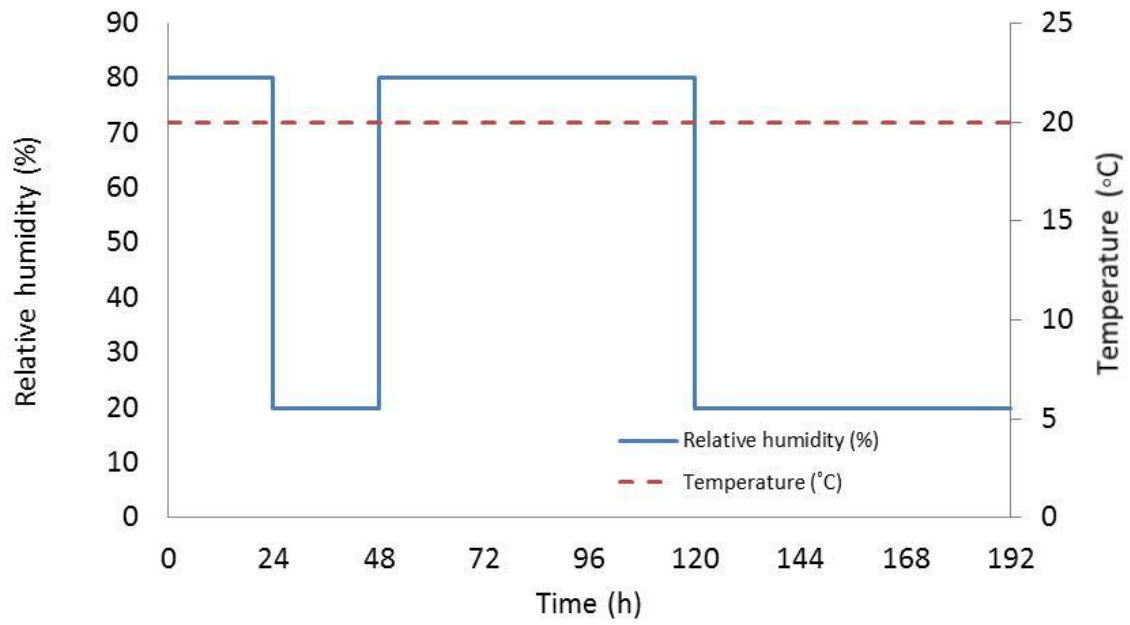


Fig 6 Relative humidity cycle used to force deformation of the wood-welded panels.

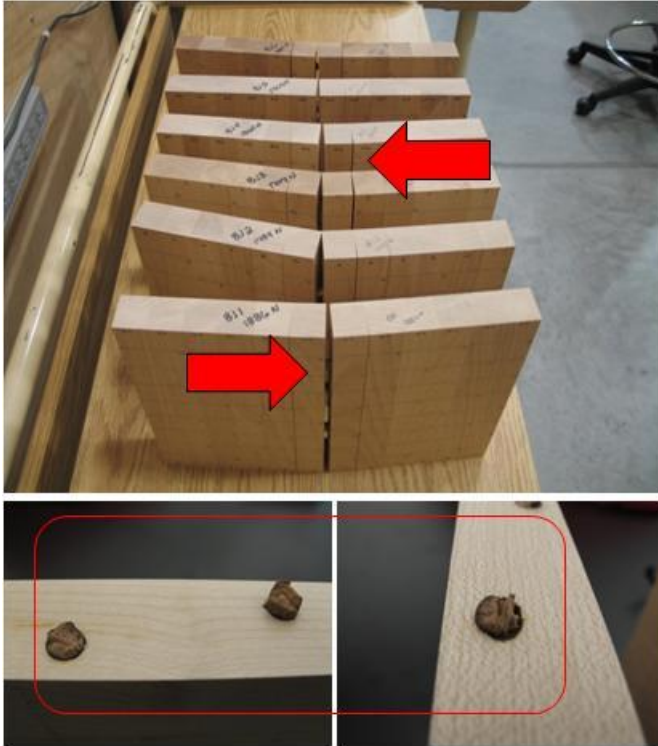


Fig 7 Failure of a wood-welded panel in the joints at the midspan or in the lamination next to it following bending tests (top picture). Fractured dowels with no slippage along the welded interface (bottom pictures).

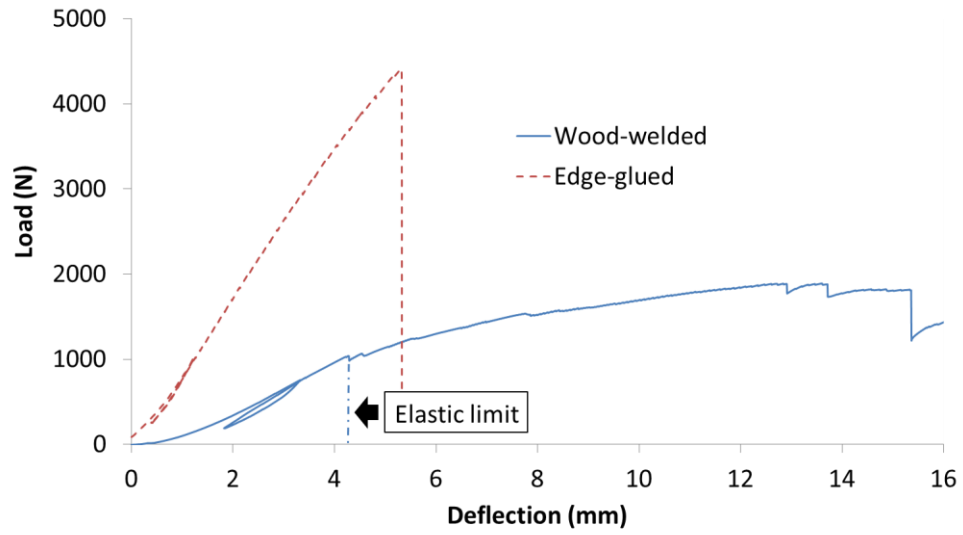


Fig 8 Typical three-point bending test load-deformation curve for yellow birch wood-welded and edge-glued panels at equilibrium.

Table 1. Load at break ( $P_{max}$ ) and slope of the straight line portion of the load deflection curve ( $\Delta F/\Delta\delta$ ) during three-point bending testing for sugar maple and yellow birch wood-welded or edge glued panels under constant or varying hygrometric conditions.

Species	Joint type	Hygrometric conditions					
		At equilibrium			After humidity cycling		
		$P_{max} \pm SE^1$	$\Delta F/\Delta\delta^2 \pm SE$ (kN mm <sup>-1</sup> )	$\delta_{max}^3 \pm SE$ (mm)	$P_{max} \pm SE$	$\Delta F/\Delta\delta^2 \pm SE$ (kN mm <sup>-1</sup> )	$\delta_{max} \pm SE$ (mm)
		(kN)			(kN)		
Sugar maple	Welded	1.70 (0.14)	0.37 (0.04)	11.1 (3.8)	2.13 (0.05)	0.45 (0.01)	9.2 (0.7)
	Glued	5.75 (0.76)	1.52 (0.05)	3.9 (1.1)	-	-	-
Yellow birch	Welded	1.79 (0.04)	0.34 (0.01)	14.0 (2.1)	1.82 (0.06)	0.34 (<0.01)	13.1 (2.4)
	Glued	5.21 (0.52)	0.98 (0.04)	6.2 (0.8)	-	-	-

<sup>1</sup>Standard error; <sup>2</sup>Linear regression of the load-deflection curve from 0.1 to 0.4 of  $P_{max}$ ; <sup>3</sup>Average deflection at failure.